



**HAL**  
open science

# Analysis of Fano-line shapes from agile resonant waveguide grating sensors using correlation techniques

Kristelle Bougot-Robin, Weijia Wen, Henri Benisty

## ► To cite this version:

Kristelle Bougot-Robin, Weijia Wen, Henri Benisty. Analysis of Fano-line shapes from agile resonant waveguide grating sensors using correlation techniques. *Optical Sensors 2013*, Apr 2013, Prague, Czech Republic. pp.UNSP 87741B, 10.1117/12.2017563 . hal-00860049

**HAL Id: hal-00860049**

**<https://iogs.hal.science/hal-00860049v1>**

Submitted on 30 Jun 2024

**HAL** is a multi-disciplinary open access archive for the deposit and dissemination of scientific research documents, whether they are published or not. The documents may come from teaching and research institutions in France or abroad, or from public or private research centers.

L'archive ouverte pluridisciplinaire **HAL**, est destinée au dépôt et à la diffusion de documents scientifiques de niveau recherche, publiés ou non, émanant des établissements d'enseignement et de recherche français ou étrangers, des laboratoires publics ou privés.



Distributed under a Creative Commons Attribution - NonCommercial 4.0 International License

# Analysis of Fano-line shapes from agile resonant waveguide grating sensors using correlation techniques

K. Bougot-Robin\*<sup>a</sup>, W.J. Wen<sup>b</sup>, H. Benisty<sup>c</sup>

<sup>a</sup>Institute for Advanced Study, Hong Kong University of Science and Technology, Clear Water Bay, Kowloon, Hong-Kong, China

<sup>b</sup>Department of Physics, Hong Kong University of Science and Technology, Clear Water Bay, Kowloon, Hong-Kong, China

<sup>c</sup>Laboratoire Charles Fabry, Institut Optique Graduate School, 2 avenue Fresnel, CNRS, Univ P Sud, 91127 Palaiseau, France

e-mail: kristelle\_robin@yahoo.fr

## ABSTRACT

The asymmetric Fano resonance lineshape, resulting from interference between background and a resonant scattering, is archetypal in resonant waveguide grating (RWG) reflectivity. Resonant profile shift resulting from a change of refractive index (from fluid medium or biomolecules at the chip surface) is classically used to perform label-free sensing. Lineshapes are sometimes sampled at discretized “detuning” values to relax instrumental demands, the highest reflectivity element giving a coarse resonance estimate. A finer extraction, needed to increase sensor sensitivity, can be obtained using a correlation approach, correlating the sensed signal to a zero-shifted reference signal. Correlation approach is robust to asymmetry of Fano lineshapes and allows more accurate determination than usual fitting options such as Gaussian or Lorentz shape fitting. Our findings are illustrated with resonance profiles from silicon nitride “chirped” RWGs operated at visible wavelengths. The scheme circumvents the classical but demanding spectral or angular scans: instead of varying angle or wavelength through fragile moving parts or special optics, a RWG structure parameter is varied. Then, the spatial reflectivity profiles of tracks composed of RWGs units with slowly varying filling factor (thus slowly varying resonance condition) are measured under monochromatic conditions. Extracting the resonance location using plain images of these “pixelated” Fano profiles allows multiplex refractive index based sensing with a sensitivity down to  $2 \times 10^{-5}$  RIU as demonstrated experimentally. This scheme based on a “Peak-tracking chip” demonstrates a new technique for bioarray imaging using a simpler set-up that maintains high performance with cheap lenses.

**Keywords:** Resonant waveguide grating – Fano lineshapes – Correlation - Refractive index sensor – Biochip imaging - Nanostructuration

## 1. INTRODUCTION

### 1.1 Resonance spatial tracking

Dielectric resonant waveguide gratings allow label-free sensing based on change in resonance response induced by effective refractive index change. Applications are bulk refractive index sensing or biological sensing of species immobilized on a chip surface.

The general shape of the resonance response is a Fano-shaped profile [1], and can be expressed by equation (1)

$$\frac{I_{\text{refl}}}{I_{\text{inc}}} \propto \frac{(q\Gamma_{\text{res}}/2 + u - u_{\text{res}})^2}{(\Gamma_{\text{res}}/2)^2 + (u - u_{\text{res}})^2} \quad (1)$$

with  $\Gamma_{\text{res}}$  the full width, and  $q$  the asymmetry parameter.

Change of resonance condition might be measured through the shift of the resonant response, for instance from spectral measurement ( $u \equiv \lambda$ ) [2,3] or angular scan ( $u \equiv \theta$ ) [4], or through the change of diffraction efficiency  $I_{refl}(u=u_0)$  measured in fixed spectro-angular optical configuration [5]. While the shift in resonance response is more robust measurement as it is based on an intensity sequence instead of one point, it however relies on costly instrumentation. For spectral based measurement, sensing in a 2D array format is ensured either using a spectro-imager [2] or tunable light source [3]. Angular sequences are measured by highly precise angular scan [4].

To combine simple instrumentation [5] and robust measurement based on near-resonance intensity sequence, we recently proposed a scheme based on spatial intensity sequence [6,7]. Instead of varying parameter through instrumentation, our scheme is based on a specially designed nanostructure with a spatial parameter  $u$  varied to scan the resonance.

Resonant response depends on layer thicknesses, etching depth, filling factor, layers refractive indexes and period. We call “tracks” the sensing area on the chip. To scan around the resonance, the waveguide structure is varied slowly along a track and a resonant profile can then be extracted from spatial information of a monochromatic picture. In this paper, we illustrate the case of filling factor variation. This choice allows both a choice compatible with 2D array sensing (change of pattern easier to control for a  $N \times P$  disposition of tracks). In Fig. 1(A), we give the resonant response for refractive indexes of the sensed medium of 1.39 and 1.4, namely for a change in refractive index of  $\Delta n = 10^{-2}$ . Fig. 1(B) gives the intensity images, as can be measured experimentally using a monochromatic set-up and illuminating the chip in resonant conditions. A scheme of a track is given in Fig. 1(C) and results in a stepwise profile as seen in Fig. 1(A) due to fabrication limitation. The discrete structures of the tracks are called « micropads » with micropads of filling factor  $f_m = d_m / \Lambda_m$ , where  $m$  is the index of the micropad.

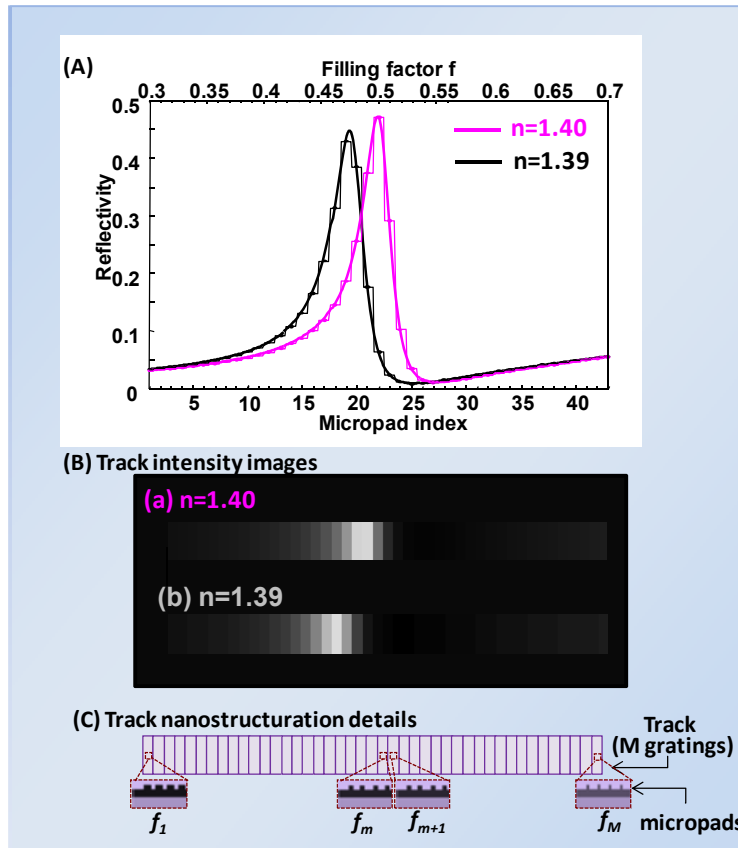


Figure 1: (A) Fano profiles for sensed media of refractive index  $n_A=1.39$  and  $n_B=1.4$  (B) Same as in (A) but in intensity scale, corresponding to measured images on a monochromatic set-up (C) Track details, with micropads of different filling factors,  $f_m = d_m / \Lambda$ , where  $d_m$  is the groove width.

## 1.2 Discrete Fano profiles

The stepwise shape of the Fano profiles is due to the discrete variation of the filling factor value between neighboring micropads of a track. Due to the small dimensions of the lines and grooves, the pattern is fabricated by electron beam lithography. For fabrication issues, the pattern can be varied only discretely. From our electron-beam lithography system, between each neighboring micropad, the groove width varies by steps of 4 nm. The chip is designed to be illuminated through the substrate so the incident direction of impinging wave on the grating is not changed by the sensed medium. Our chip is designed to perform sensing in green with excitation close from normal incidence. The waveguide structure is varied along the long dimension of the track. It is made with a low refractive index transparent substrate (here borosilicate glass), covered by high-index guiding layer, here silicon nitride with  $n \sim 2$ , with thickness  $0.28\Lambda$ , where  $\Lambda$  is the period of the grating. To ensure close from normal incidence imaging we choose a period of  $\Lambda = 450$  nm. The resulting filling factor variation  $\Delta f = 4/450 \text{ nm} = 0.0089$ .

For a filling factor span (0.3-0.7), it corresponds to a number of  $M = 43$  micropad units, which allows to span a refractive index range (1.3-1.5) with our present structure [6]. A spatial shift of the micropad of maximum diffraction efficiency towards higher filling factor is observed as refractive index of the sensed solution increases, or as mass coverage on biochip surface increases in the case of biosensing.

On a whole chip area, several tracks may be placed on the same surface. Taking into account space issues on the chip support, as well as memory in term of image acquisition, few tens or even hundred of tracks may be sensed in parallel. This therefore makes such spatial tracking principle an interesting direction for multiplex sensing.

## 2. FANO LINESHAPE ANALYSIS

### 2.1 Correlation analysis

For sensing purpose, it is necessary to quantify the shift of the resonant response, and then deduce the change of refractive index (or the amount of biomolecules) at the chip surface.

In a recent study, we demonstrated that correlation analysis was robust to Fano lineshape asymmetry and gave better accuracy than usual fitting models (namely Gauss and Lorentz). In Fig.2, we illustrate the shift calculation using correlation analysis.

We call  $S$  the signal to analyze and  $S_{ref}$  the reference signal. Here the signal images consist in 2D matrix, of dimensions  $D_x \times M D_y$ , where  $M$  is the number of micropad per track and  $D_x$  and  $D_y$  are the number of pixels spanning a micropad in both directions.

Note that the number of pixels in the vertical direction might be  $D_y = 1$ , and therefore our correlation analysis model can be applied to any Fano lineshapes signal. This shift in micropad unit is considered as proportional to the refractive index change at the chip surface. For a large refractive index span, a curvature is observed and a calibration might be necessary to determine the peak shift.

Except from parasitic contributions the  $D_x$  lines ideally have the same signal, and we therefore calculate the correlation on each of the lines between the signal and the reference images and average over the different lines. The difference between the lines may have optical origins (for instance distortion) or be due to fabrication variability. Noise contribution is also different on each of the pixel  $(i, j)$ .

The correlation function can be expressed as follow:

$$C(\Delta j) = D_x^{-1} \sum_j \sum_i \bar{S}(i, j) \otimes \bar{S}_{ref}(i, j) \quad (1)$$

To increase the precision of this correlation beyond the micropad unit and perform sensitive sensing, meaning have a precise determination of the position of the resonance, we calculate the centroid of the correlation function after correcting it from its average and bringing it at a high power exponent  $k$ . This operation serves as limiting tail contribution in our determination.

The corresponding correlation function  $C'$  is given by equation (2):

$$C'^k = (C - \langle C^2 \rangle)^k \quad (2)$$

In this paper, we use an exponent  $k=10$ . The spatial shift of the track profile may be quantified in micropad unit  $\Delta m$ , this value being used to determine an analyte refractive index or a bilayer thickness in the case of biosensing.

$$\Delta j_{sensed} = \sum \Delta j C^{*k}(\Delta j) / \sum C^{*k}(\Delta j) \quad (3)$$

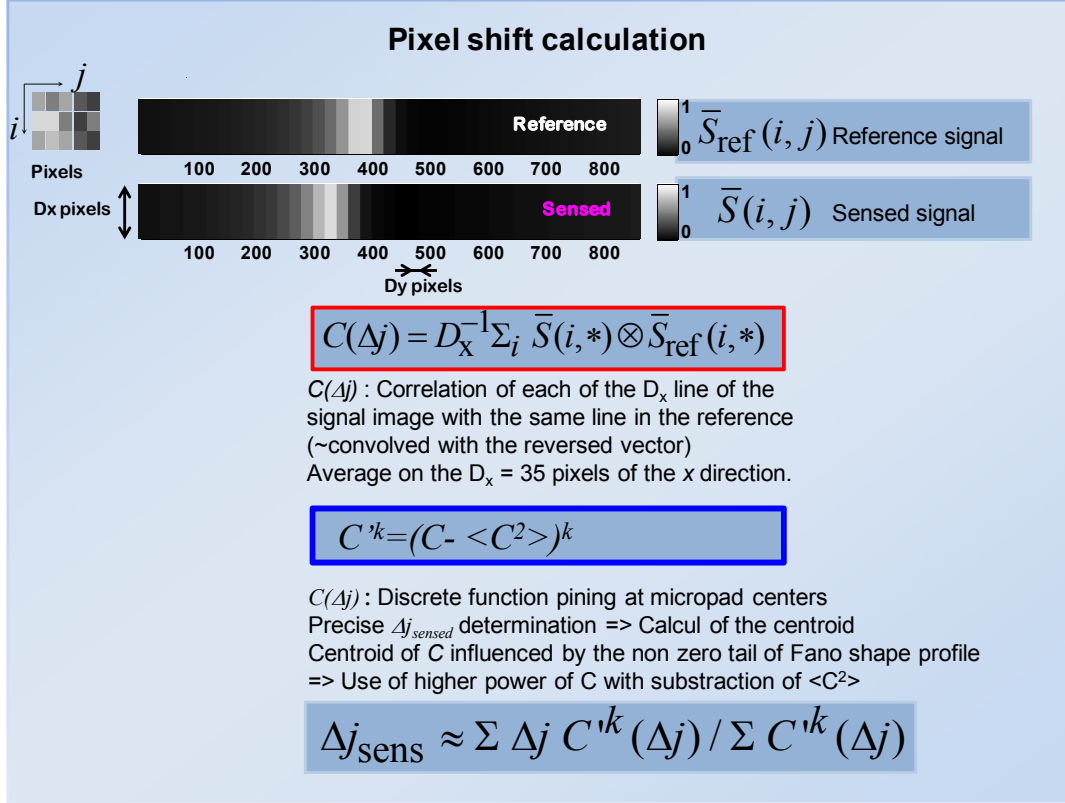


Figure 2: Correlated images and pixel shift calculation

## 2.2 Comparison to usual fitting models

Due to their asymmetry, Fano profiles are not easy to cope with [8-9]. For low discretization such as the profiles studied in this paper (only 4 points at half maximum to determine peak position), fitting to known curves such as Gauss or Lorentz gives poor accuracy [7], while correlation analysis is more robust to such asymmetric profiles.

## 2.3 Robustness to noise and other optical effects

We also studied robustness of correlation analysis with contributions such as noise or geometry variation (for instance due to inhomogeneities in fabrication, or other optical origin such as distortion) [7].

This study was realized by adding large Gaussian noise contribution on each of the pixels. A constant noise  $\bar{S}_N$  and a photon noise contributions were introduced in the model. Through successive simulations, we demonstrated that the determination of shift position was robust to such noise contributions.

We then studied the robustness to aberrations of different origins, for instance optical distortion or as observed experimentally fabrication variability, due to variable exposure in the electron beam lithography process. This study using a realistic model supported the robustness of correlation analysis to such contributions.

### 3. EXPERIMENTAL RESULTS

#### 3.1 Experiment

We here present refractive index sensing for low refractive index span from 1.333 to 1.337 by step  $\Delta n=10^{-3}$  and study the limit sensitivity. We use a chip array of  $2 \times 1$  tracks, where one serves as reference (for instance to correct from mechanical instabilities contributions) while on the other track, media with varying refractive index are circulated. To insure maximum stability as well as avoid thermo-optic effect, the media are circulated by using syringe pump with a flow rate of  $150 \mu\text{L}/\text{min}$ . We also allow the sample to reach the chamber with enough subsequent time for stabilization. A scheme of the experimental process is given in Fig. 3. Pictures are taken under in resonant condition with an incident light of wavelength  $\lambda=545 \text{ nm}$  and angle  $\theta=18^\circ$  with TM polarization. The spectral resolution is of  $\Delta\lambda=0.1 \text{ nm}$ , and the angular resolution is of  $\Delta\theta=0.1^\circ$ .

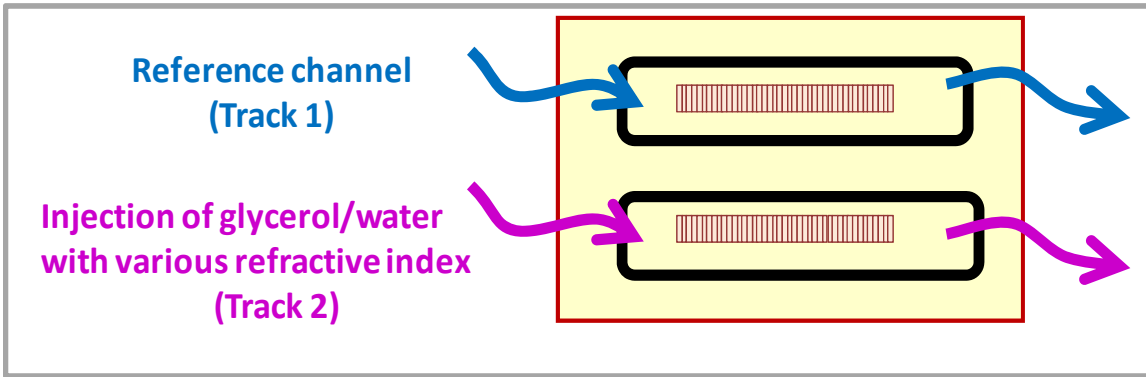


Figure 3: Scheme of the experiment: a chip of  $2 \times 1$  track is imaged in resonant condition. One track serves as reference, and on the other one media of different refractive index are circulated. Pictures are acquired for each media.

#### 3.2 Sensitive sensing

To obtain solutions of different refractive index, we use water/glycerol solution with different composition. Pictures of the tracks for different media are reported in Fig.4(A) together with one of the reference track picture. The corresponding profiles averaged over the  $x$  dimension, with  $D_x = 41$  pixels are given in Fig. 4(B). A shift of the profiles towards higher filling factor values is observed on the profiles. Micropads dimensions are of  $90 \mu\text{m} \times 200 \mu\text{m}$ , with a space of  $10 \mu\text{m}$  between neighboring micropads.

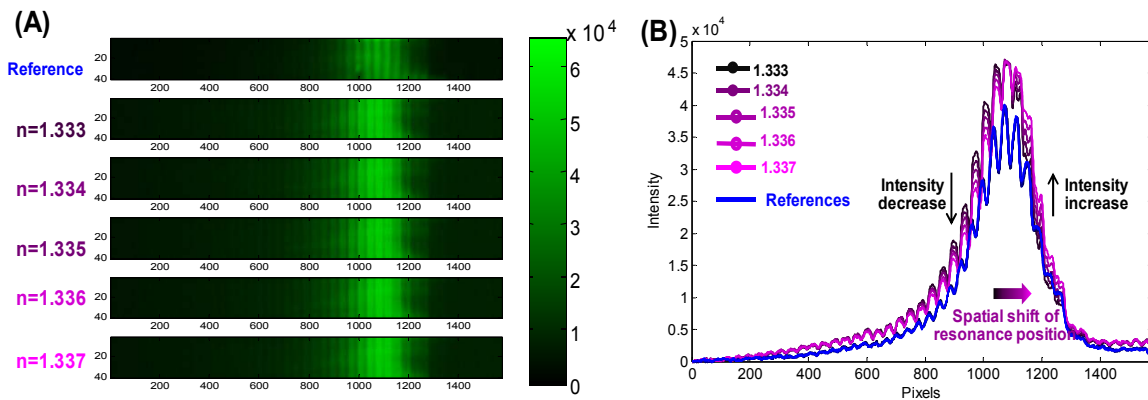


Figure 4: (A) Monochromatic pictures for different media of index from 1.333 to 1.337. The resonance position is shifted towards micropads of higher filling factors as the refractive index of the sensed media increases. (B) Corresponding track profiles averaged on the  $D_x$  pixels along the track.

To determine maximum position, we use correlation analysis. In Fig. 5 (A), we present the obtained peak shift. The local trend is linear and we report this linear fit with black line. The difference between the fit and the experimental value is reported in Fig. 5(B). The error in peak position correspond to a refractive index  $\Delta n=2\times 10^{-5}$ . This demonstrates good sensitivity of our technique and opens directions towards numerous applications, including bioarray imaging. Indeed, from refractive index experiments, we already demonstrated sensitivity of the order of  $\Delta n\sim 2\times 10^{-5}$  RIU. Induced spatial shift would be roughly the same than for a biological layer of 20 pg/mm<sup>2</sup> on the chip surface in aqueous solution. Therefore, our technique sensitivity is also compatible with real-time hybridisation experiments.

In our previous work, we demonstrated biological application by using a single probe and different concentration of analytes. To sense different analytes in parallel, different probes might be immobilised on different as we successfully did in our first biological demonstration [7]. Taking into account tracks and picture dimensions, few tens of tracks might be measured at the same time, thus allowing good parallelism for many applications.

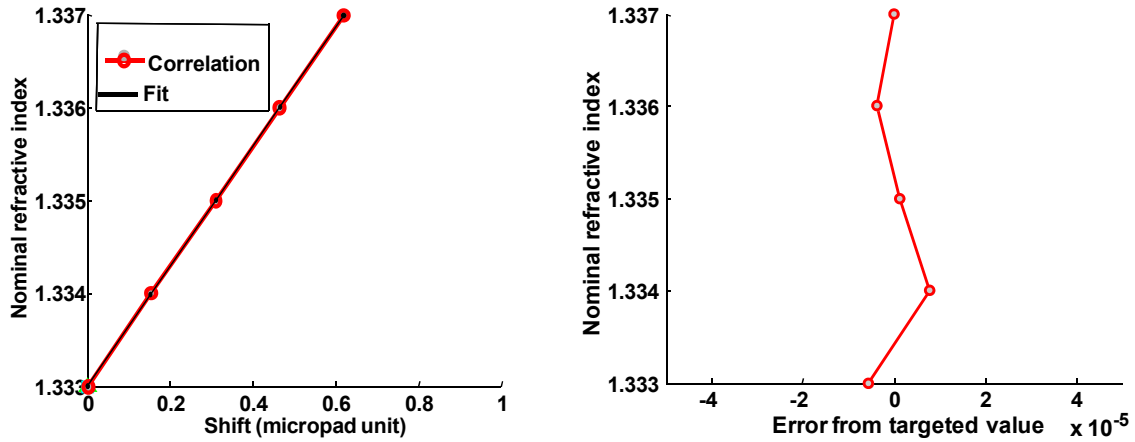


Figure 5: (A) Peak shift determined using correlation analysis (B) Error from linear position determination, giving a precision of  $2\times 10^{-5}$  in refractive index accuracy.

#### 4. Conclusion

We presented here a technique combining advantages of RWGs based sensing to simple imaging instrumentation. For robustness and sequence based measurement, we integrate the profile dimension inside the chip. Both multiplex and sensitivity aspects have been considered, demonstrating here a new method for self-reference refractive index sensing or bioarray imaging. The peak position was determined using image correlation analysis, which demonstrated robustness to Fano lineshape asymmetries, as well as other parasitic contributions such as noise or other optical effect. Fano lineshapes parameters are not trivial to determine from experimental data, and our peak shift determination technique might be extended to other resonance curves analysis. Our demonstration was realised in visible, but other domain of wavelength may also be of interest. Moreover, as additional advantages in comparison to plasmon based, multipolarisation studies are also possible. This gives our new technique large potential for sensitive sensing.

#### Acknowledgment

The electron beam lithography project supported by University Grants SEG\_HKUST10. The project is supported by RGC grant 604710 and RPC11SC01.

## REFERENCES

- [1] Fano, U. "Effects of Configuration Interaction on Intensities and Phase Shifts" *Phys. Rev.* 124, 1866–1878 (1961).
- [2] Li, P. Y., Lin, B., Gerstenmaier, J. and Cunningham B. T., "A new method for label-free imaging of biomolecular interactions," *Sens. Act. Chem.* 99, 6-13 (2004).
- [3] Ferrie, A.M., Wu Q., and Fang Y. "Resonant waveguide grating imager for live cell sensing" *Appl. Phys. Lett.* 97, 223704 (2010).
- [4] George, S. Block, I.D. , Jones, S.I., Mathias, P.C., Chaudhery, V., Wu, H.Y., Vuttipittayamongkol, P., Vodkin, L. and Cunningham, B.T. "Label-free prehybridization DNA microarray imaging using photonic crystals for quantitative spot quality analysis," *Anal. Chem.* 82, 8551-8557 (2010).
- [5] Bougot-Robin, K., Reverchon, J-L., Fromant, M., Mugheri, L., Plateau, P. and Benisty, H., "2D label-free imaging of resonant grating biochips in ultraviolet", *Opt. Express* 18, 11472-11482 (2010)
- [6] Bougot-Robin, K., Li, S., Zhang, Y., Hsing, I.M., Benisty, H., Wen, W. "'Peak Tracking Chip' for Label-Free Optical Detection of Bio-Molecular Interaction and Bulk Sensing", *The Analyst* 137(20), 4785- 4794 (2012)
- [7] Bougot-Robin, K., Wen W., Benisty, H. "Resonant waveguide sensing made robust by on-chip peak tracking through image correlation", *Biomedical Optics Express* 3(10), 2436-3451(2012).
- [8] Fang, T.K. Chang, T. N. "Determination of profile parameters of a Fano resonance without an ultrahigh-energy resolution" *Phys. Rev. A* 57(6) (1998).
- [9] Liu, X. J., Huang, Y.P., Zhu, L.F., Yuan, Z.S., Li,W.B., Xu, K.Z., "Numerical determination of profile parameters for Fano resonance with definite energy resolution" *Nucl. Instr. Meth. Phys. Res.* 508(3), 11 448–453 (2003).